

Multifractal analyses of daily rainfall time series in Pearl River basin of China

Zu-Guo Yu^{1,2}, Yee Leung^{3*}, Yongqin David Chen³, Qiang Zhang⁴, Vo Anh² and Yu Zhou¹

¹ Hunan Key Laboratory for Computation and Simulation in Science and Engineering and
Key Laboratory of Intelligent Computing and Information Processing of Ministry of Education,
Xiangtan University, Xiangtan, Hunan 411105, China.

²School of Mathematical Sciences, Queensland University of Technology,
GPO Box 2434, Brisbane, Q4001, Australia.

³Department of Geography and Resource Management, and Institute of Environment,
Energy and Sustainability, The Chinese University of Hong Kong, Hong Kong, China.

⁴Department of Water Resources and Environment, and Key Laboratory of
Water Cycle and Water Security in Southern China of Guangdong High Education Institute,
Sun Yat-sen University, Guangzhou 510275, China.

Abstract

The multifractal properties of daily rainfall time series at the stations in Pearl River basin of China over periods of up to 45 years are examined using the universal multifractal approach based on the multiplicative cascade model and the multifractal detrended fluctuation analysis (MF-DFA). The results from these two kinds of multifractal analyses show that the daily rainfall time series in this basin have multifractal behavior in two different time scale ranges. It is found that the empirical multifractal moment function $K(q)$ of the daily rainfall time series can be fitted very well by the universal multifractal model (UMM). The estimated values of the conservation parameter H from UMM for these daily rainfall data are close to zero indicating that they correspond to conserved fields. After removing the seasonal trend in the rainfall data, the estimated values of the exponent $h(2)$ from MF-DFA indicate that the daily rainfall time series in Pearl River basin exhibit no long-term correlations. It is also found that $K(2)$ and elevation series are negatively correlated. It shows a relationship between topography and rainfall variability.

Key words: Daily rainfall time series; multifractal property; universal multifractal model; multifractal detrended fluctuation analysis.

1 Introduction

Rainfall is one of the most important variables studied because its non-homogenous behavior in event and intensity, leading to drought, water runoff and soil erosion with negative environmental

*Corresponding author, email: yeeleung@cuhk.edu.hk

and social consequences [1,2]. Analysis and modelling of rainfall are significant research problems in applied hydro-meteorology [3]. Rainfall time series often exhibit strong variability in time and space.

Rainfall also exhibits scaling behavior in time and space (e.g. [3-7]). There is thus a need to characterize and model rainfall variability at a range of scales which goes beyond the scales that can be directly resolved from observations [8]. Investigation of the existence of fractal behavior in rainfall processes has been an active area of research for many years [9]. Some recent experiments have shown that scale invariance, in time and space, does exist in rainfall fields [10]. Olsson *et al.* [11] investigated the rainfall time series by calculating the box and correlation dimensions via a monodimensional fractal approach (simple scaling). Their results indicate scaling but with different dimensions for different time aggregation periods. Hence the investigated rainfall time series display a multidimensional fractal behavior. Venugopal *et al.* [12] employed the wavelet-based multifractal analysis to reexamine the scaling structure of rainfall over time. Molnar and Burlando [13] used the exponent of correlation function, a multifractal parameter, to study the seasonal and spatial variabilities. Using 2-dimensional Fourier series analysis and spectral analysis, Boni *et al.* [14] proposed a methodology to study the estimated index factor for rainfall in mountainous regions. During the past two decades, stochastic models of rainfall have increasingly exploited the property of multifractal scale invariance, resulting in multifractal models that are more advantageous over conventional models in rainfall representations [15-17].

The multiplicative cascade model has been widely used to study the multifractal properties of the rainfall data (e.g. [2, 4-8, 17-29]). Schertzer and Lovejoy [4] showed that statistically scaled invariant processes are stable and converge to some universal attractor, and thus can be defined by a small number of relevant parameters, specifically three with the universal multifractal framework.

The simple multifractal analysis (MFA) is based upon the standard partition function multifractal formalism [30], developed for the multifractal characterization of normalized, stationary measurements. Unfortunately, this standard formalism does not give correct results for non-stationary time series that are affected by trends or that cannot be normalized [31]. Thus, two generalizations of simple MFA were developed. One is the wavelet-based MFA which has been used to study rainfall data (e.g. [12]). Another generalization is the multifractal detrended fluctuation analysis (MF-DFA) [31] which is an extension of the standard detrended fluctuation analysis (DFA) introduced by Peng *et al.* [32,33]. DFA can be employed to detect long-range correlations in stationary and noisy nonstationary time series. It intends to avoid the unravelling of spurious correlations in time series. The DFA method has been successfully applied to problems in fields such as DNA and protein sequences (e.g. [32,34,35]) and hydrology (e.g. [36-40]). The MF-DFA is a modified version of DFA for the detection of multifractal properties of time series. It renders a reliable multifractal characterization of nonstationary time series encountered in phenomena such as those in geophysics [31, 37, 38, 41-46]. The MF-DFA has also been successfully applied to problems in hydrology (e.g. [37-39]). The relationship between topography and rainfall variability is a very important issue in the study of rainfall.

Our work in this paper focuses on the multifractal properties of daily rainfall time series and

possible relationships between the multifractal exponents and landscape properties. We use the universal multifractal model (UMM) proposed by Schertzer and Lovejoy [4] to fit the multifractal moment function $K(q)$ of the rainfall data and propose a method to estimate the parameters. We also adopt the MF-DFA approach to detect the correlation and multifractal properties of daily rainfall data in this paper.

As the largest watershed in South China, the Pearl River (Zhujiang in Chinese) delta is a composite drainage basin with a total area of 45.4×10^4 km², consisting of three major rivers (i.e., West River, North River, and East River) and several independent rivers in the downstream and delta regions (see Figure 1). The Asian monsoon and moisture transport are the important influencing factors on precipitation patterns in this region. Given its large size and dominance of a sub-tropical humid monsoon climate, the Pearl River basin is under the influence of rainfall variability which is a highly complicated process in space and time. Zhang et al. [47] reported an increased high-intensity rainfall over the basin in conjunction with the decreased rainy days and low-intensity rainfall. It was also found that the abrupt changes of the precipitation totals (for annual, winter, and summer precipitation) occurred in the late 1970s, 1980s, and early 1990s, and the precipitation intensity basically increased after the change points [47, 48]. In this paper, we study the daily rainfall data over the period from 1 January 1960 to 31 December 2005 at 41 locations in Pearl River basin using the UMM and MF-DFA methods. Parameters from the above MFAs are used to infer the spatial relationship of rainfall in Pearl River basin of China.

2 Multifractal analyses

2.1 Universal multifractal approach based on the multiplicative cascade model

Let $T(t)$ be a positive stationary stochastic process at a bounded interval of \mathbf{R} , assumed to be the unit interval $(0, 1)$ for simplicity, with $E(T(t)) = 1$ (For a time series x_i , $i = 1, \dots, L$, we can define $t_i = i/L$, and $T(t_i) = x_i / (\sum_{k=1}^L x_k)$). The smoothing of $T(t)$ at scale $r > 0$ is defined as $T_r(t) = \frac{1}{r} \int_{t-r/2}^{t+r/2} T(s) ds$. We consider the processes $X_r(t) = \frac{T_r(t)}{T_1(t)}$, $t \in [0, 1]$. The empirical multifractal function $K(q)$ can be defined as the power exponents if the following expectation behaves like [49]

$$E(X_r^q(t)) \propto r^{K(q)}. \quad (1)$$

If we consider smoothing at discrete scales r_j , $j = 1, 2, \dots$, then from Eq. (1), the empirical $K(q)$ function (denoted as $K_d(q)$) for the data can be obtained by

$$K_d(q) = \lim_{j \rightarrow \infty} \frac{\ln E(X_{r_j}^q)}{-\ln r_j}. \quad (2)$$

Hence the empirical $K(q)$ function $K_d(q)$ can be estimated from the slopes of $E(X_r^q)$ against the scale ratio $1/r$ in a log-log plane. In this paper, we adopt Eq. (2) to obtain $K_d(q)$ of our rainfall data. If the curve $K_d(q)$ versus q is a straight line, the data set is monofractal. However, if this curve is convex, the data set is multifractal [30].

The universal multifractal model (UMM) proposed by Schertzer and Lovejoy [4] assumes that the generator of multifractals was a random variable with an exponentiated extremal Lévy distribution.

Thus, the theoretical scaling exponent function $K(q)$ for the moments $q \geq 0$ of a cascade process is obtained according to [4, 18, 28, 29]:

$$K(q) = qH + \begin{cases} C_1(q^\alpha - q)/(\alpha - 1), & \alpha \neq 1, \\ C_1q \log(q), & \alpha = 1, \end{cases} \quad (3)$$

in which the most significant parameter $\alpha \in [0, 2]$ is the Lévy index, which indicates the degree of multifractality (i.e. the deviation from monofractality). $C_1 \in [0, d]$, with d being the dimension of the support ($d = 1$ in our case), describes the sparseness or inhomogeneity of the mean of the process [28]. The parameter H is called the non-conservation parameter since $H \neq 0$ implies that the ensemble average statistics depend on the scale, while $H = 0$ is a quantitative statement of ensemble average conservation across the scales (e.g., [29]).

Although the double trace moment (DTM) technique [50, 51] has been widely used to estimate the parameters H , C_1 and α in geophysical research, it is complicated and the goodness of fit of the empirical $K(q)$ functions depends on that of exponent β of the power spectrum, and sometimes the fitting of $K(q)$ is not satisfactory (e.g., [19, 28, 29]). In this paper, we adopt a method in [52] and is similar to that proposed in [49]. If we denote $K_T(q)$ the $K(q)$ function defined by Eq. (3), we estimate the parameters by solving the least-squares optimization problem [52]

$$\min_{H, C_1, \alpha} \sum_{j=1}^J [K_T(q_j) - K_d(q_j)]^2. \quad (4)$$

In our analysis, we take $q_j = j/3$ for $j = 1, 2, \dots, 30$.

2.2 Multifractal detrended fluctuation analysis

We outline the MF-DFA procedure used here according to the procedure described in [31].

Suppose that x_k is a series of length N . First we determine the 'profile' $Y(i) = \sum_{k=1}^i [x_k - \langle x \rangle]$, $i = 1, \dots, N$, where $\langle x \rangle$ is the mean of $\{x_k\}$. For an integer $s > 0$, we divide the profile $Y(i)$ into $N_s = \text{int}(N/s)$ non-overlapping segments of equal lengths s , where $\text{int}(N/s)$ is the integer part of N/s . Since the length N of the series is often not a multiple of the timescale s under consideration, there may remain a slack at the end of the profile. In order not to disregard this short part of the series, the same procedure is repeated starting from the opposite end. Thus, $2N_s$ segments are obtained altogether. Now we can calculate the local trend for each of the $2N_s$ segments by a least squares linear fit of the series, then determine the variance $F^2(s, \nu)$ for $\nu = 1, \dots, 2N_s$ [31]. Then the q th-order fluctuation function is defined as $F_q(s) = \left[\frac{1}{2N_s} \sum_{\nu=1}^{2N_s} (F^2(s, \nu))^{q/2} \right]^{1/q}$, where $q \neq 0$. Finally we determine the scaling behavior

$$F_q(s) \propto s^{h(q)}. \quad (5)$$

of the fluctuation functions by analyzing the log-log plot of $F_q(s)$ versus s for each value of q . The exponent $h(q)$ is commonly referred to as the generalized Hurst exponent. The MF-DFA is suitable for both stationary and nonstationary time series [31]. We denote \tilde{H} the Hurst exponent of time series. The range $0.5 < \tilde{H} < 1$ indicates long memory or persistence; and the range $0 < \tilde{H} < 0.5$

indicates short memory or anti-persistence. For uncorrelated series, the scaling exponent \overline{H} is equal to 0.5. Assuming the setting of fractional Brownian motion, Movahed *et al.* [53] proved the relation $\overline{H} = h(2) - 1$ between \overline{H} and the exponent $h(2)$ for small scales. In the case of fractional Gaussian noise, it was shown that $h(2) = \overline{H}$ [53]. Hence we can use the value of \overline{H} calculated from $h(2)$ to detect the nature of memory in time series under the assumption of fractional Gaussian noise or fractional Brownian motion.

In the case of a power law, the power spectrum $S(f)$ is related to the frequency f by $S(f) \propto (1/f)^\beta$. The exponents $h(2)$ and β are related to each other by the equation $h(2) = (1+\beta)/2$ [36,54]. As pointed out by Lovejoy *et al.* [26], the relationship between mass exponent $\tau(q)$, which is based upon the standard partition function multifractal formalism [30], and $K(q)$ is

$$\tau(q) = (q - 1) - K(q), \quad (6)$$

for 1-dimensional data. For a conservative process, Koscielny-Bunde *et al.* [39] pointed out the relationship between $h(q)$ and $K(q)$ as

$$qh(q) = qh(1) - K(q). \quad (7)$$

By combining Eqs. (6) and (7), we get [55]

$$\tau(q) = q(h(q) - h(1)) + q - 1. \quad (8)$$

3 Results and discussion

In this study, we apply the above methods to examine the multifractal properties of daily rainfall data in Pearl River basin over time as a regional case study. At each of the 41 stations in Pearl River basin, daily rainfall data over the period from 1 January 1960 to 31 December 2005 consist of 16,802 observations. The information on location and elevation of the 41 stations in Pearl River basin is given in Table 1 (we list the stations according to the decreasing order of their elevations). According to the elevation, we can divide the stations into three groups (Group 1 with elevation higher than 1000m, Group 2 with elevation between 200m to 1000m, Group 3 with elevation lower than 200m). The daily rainfall data of Station 56691 and Station 57922 (in the Pearl River basin) over the entire study period are shown in Figure 2 as examples.

First, we computed the empirical $K(q)$ curves of all daily rainfall data via Eq.(2) by taking values for r_j from 0.0010 to 0.056 (corresponding to time scale from 180-960 days) for data in Pearl River basin because the power-law relation in Eq.(2) in these time scale ranges becomes linear. An example for obtaining the empirical $K(q)$ curves is given in Figure 3. The empirical $K(q)$ curves of the rainfall data in two stations are shown in Figure 4 (the dotted lines) as examples. We observed that all the empirical $K(q)$ curves of the rainfall data in all stations are not straight lines (i.e. are convex lines) like those in Figure 4. This suggests that all daily rainfall time series have multifractal behavior in the time scale range from 180 to 960 days. In order to use the UMM (i.e. Eq. (3)) to fit the empirical $K(q)$ curves, we use the function *fminsearch* in MATLAB to solve the optimization problem (Eq.(4)) and obtain the estimates of parameters H , α and $C1$ (we set 0.5, 0.5, 0.5 as

the initial values of these three parameters, respectively). The estimated values of parameter α for stations in the Pearl River basin are given in Table 1. We found that the theoretical $K(q)$ curves based on the UMM fit exceedingly well the empirical $K(q)$ curves of the rainfall data in all stations. We plot two fitted theoretical $K(q)$ curves in Figure 4 (the continuous lines) as illustrations. From the estimated values of H , C_1 and α , we find that $H \in [-0.0459, 0.0196]$ with mean value -0.0085 ± 0.0126 , $C_1 \in [0.0867, 0.2665]$ with mean value 0.1631 ± 0.0385 , and $\alpha \in [0.6213, 1.6072]$ with mean value 1.0236 ± 0.2141 for stations in Pearl River basin. The values of H with mean value -0.0085 ± 0.0126 for these daily rainfall data are close to zero, indicating that they correspond to conserved fields which is consistent with previously published results (e.g., [26-29]). Since the values of α are fairly large (far from the monofractal value of zero), it again confirms that all daily rainfall time series in Pearl River basin have multifractal behavior in the time scale range from 180 to 960 days. The values of C_1 with mean value 0.1631 ± 0.0385 indicate that the conserved multifractal daily rainfall is not too sparse [18], which can be compared with previously published results [19,23].

Second, we employed the MF-DFA to analyze the rainfall data. There are usually seasonal variations in rainfall data. In order to get the long term correlations correctly, the data need to be deseasonalized before we can perform the MF-DFA [39, 40, 56-58]. In this paper, the deseasonalized rainfall z_i ($i = 1, 2, \dots, N$, N is the total number of data points) are obtained by subtracting the mean daily rainfall \bar{x}_i from the original rainfall x_i and normalized by variance at each calendar date [40, 56-58], i.e.,

$$z_i = (x_i - \bar{x}_i) / (\overline{x_i^2} - \bar{x}_i^2). \quad (9)$$

The deseasonalized rainfall was analyzed with MF-DFA. Here we calculated $h(q)$ over the scale range of 10 to 87 days for all values of q because the log-log plot of $F_q(s)$ versus s for each value of q in this time scale range becomes linear. An example for obtaining the empirical $h(q)$ curve is given in Figure 5. The empirical $h(q)$ curves of the rainfall data in two stations are shown in Figure 6 as examples. We observed that all the empirical $h(q)$ curves of the rainfall data in all stations we considered are not straight lines (i.e. are convex lines) like those in Figure 6. This suggests that all daily rainfall time series have multifractal behavior in the time scale range from 10 to 87 days. Usually the value of $\Delta h(q)$ (defined as $\max\{h(q)\} - \min\{h(q)\}$) is used to characterize the multifractality of time series. The estimated values of $h(1)$, $h(2)$ and $\Delta h(q)$ for stations in Pearl River basin are given in Table 1. From Table 1, we find that $h(2) \in [0.5248, 0.6436]$ with mean value 0.5891 ± 0.0275 , $\Delta h(q) \in [0.3724, 0.8851]$ with mean value 0.5681 ± 0.1210 for stations in Pearl River basin. The values of $\Delta h(q) \in [0.3724, 0.8851]$ obtained by us with mean value 0.5681 ± 0.1210 (far from the monofractal value of zero) for stations in Pearl River basin again confirms that all daily rainfall time series in Pearl River basin have multifractal behavior in the time scale range from 10 to 87 days. It was reported that the scaling exponents of rainfall obtained by DFA for the intermediate time scales (10.0 to 100.0-300.0 days) range in values from 0.62 to 0.89 [36] without removing the seasonal trend in the data. Later on, after removing the seasonal trend in the rainfall data, Kantelhardt *et al.* [38] found that most precipitation records exhibit no long-term correlations ($h(2) \approx 0.55$), the mean value is $h(2) = 0.53 \pm 0.04$. The values of $h(2) \in [0.5248, 0.6436]$ obtained by us with mean value 0.5891 ± 0.0275 for stations in Pearl River basin consists with the result that

precipitations are mainly uncorrelated reported in [38].

It is also interesting to test the relationship between $K(2)$ and $h(2)$ given by Eq. (7), i.e. whether $K(2) = 2[h(1) - h(2)]$ holds. We denote $K'(2)$ to be $2[h(1) - h(2)]$. The estimated values of $K'(2)$ for stations in Pearl River basin are given in Table 1. From Table 1, we find that $K'(2) \in [0.1960, 0.5300]$ with mean value 0.2980 ± 0.0728 for stations in Pearl River basin. We find from Table 1 that the values of $K'(2)$ are quite different from those of $K(2)$, this because that they are estimated for different time scale ranges.

Last, we want to see whether the parameters from these MFAs of daily rainfall can reflect some spatial or geographical characteristics of the stations in Pearl River basin. In other words, we would like to explore the spatial dimension of rainfall variability in the basin. In particular, we are interested in finding out whether rainfall variations over time are related to, for example, the topography of the basin. A scrutiny of the parameters H , α and C_1 in UMM, $K(2)$ in the $K(q)$ curves, and $h(2)$ from MF-DFA show that there exhibit some correlations between rainfall regime and basin characteristics such as topography. In fact, we found that the parameter $K(2)$, which is related to the correlation dimension $D(2)$ via $D(2) = 1 - K(2)$, of the daily rainfall data reflects some spatial and geographical features of the stations in the basin. First, $K(2)$ and elevation series are negatively correlated. The value of the correlation coefficient between $K(2)$ and elevation is up to -0.4995 in the Pearl River basin as shown in Figure 7. The possible trend is that the higher the elevation at which a station is located, the smaller the value of $K(2)$ becomes and the closer it is to 0.0 (so also the larger the value of $D(2)$ becomes and the closer it is to 1.0). According to the elevation, we can divide the stations into three groups (Group 1 with elevation higher than 1000m, Group 2 with elevation between 200m to 1000m, Group 3 with elevation lower than 200m). We found that $K(2)$ of Group 1 have mean value 0.1927 ± 0.0110 , that of Group 2 have mean value 0.2000 ± 0.0181 and that of Group 3 have mean value 0.2155 ± 0.0202 . One can see that the mean value of $K(2)$ of these three groups become larger with decreasing of elevation. We also notice that rainfall stations at higher elevations in the northwestern side of the basin similarly tend to have smaller $K(2)$ values in comparison with stations at lower elevations in the southeastern side. Using the wavelet analysis on the monthly precipitation data in Pearl River basin, Niu [59] recently found that, apart from the high variability for the less than 1-year period, the high wavelet power in the dominant band (0.84-4.8 years) for the first and second modes (especially for northwest part and east part of Pearl River basin) reflects long-term precipitation variability. Niu [59] explained that the northwest region has the highest altitudes, and therefore it is influenced by the topographic rain shadow with respect to the prevailing storm tracks; while the east region is close to the South China Sea which is subjected to convective movement of water by semitropical hurricanes and typhoons.

4 Conclusion

Multifractal analysis is a useful method to characterize the heterogeneity of both theoretical and experimental fractal patterns. As a regional case study, numerical results obtained from the universal multifractal approach and MF-DFA on the daily rainfall data in Pearl River basin show that these

time series have multifractal behavior in two different time scale ranges. It is found that the empirical $K(q)$ curves of the daily rainfall time series can be fitted very well by the UMM. The estimated values of H for these daily rainfall data are close to zero, indicating a correspondence to the conserved fields.

After removing the seasonal trend in the rainfall data, the estimated values of $h(2)$ indicate that the daily rainfall time series in Pearl River basin exhibit no long-term correlations.

It is found that $K(2)$ and elevation series are negatively correlated. It shows a relationship between topography and rainfall variability.

Acknowledgements

This project was supported by Geographical Modelling and Geocomputation Program under the Focused Investment Scheme of The Chinese University of Hong Kong, and the Earmarked grant CUHK405308 of the Research Grants Council of the Hong Kong Special Administrative Region; the Natural Science Foundation of China (Grant no. 11071282 and 11371016), the Chinese Program for Changjiang Scholars and Innovative Research Team in University (PCSIRT) (Grant No. IRT1179), the Research Foundation of Education Commission of Hunan Province of China (grant no. 11A122), the Lotus Scholars Program of Hunan province of China.

References

- [1] G.R. Walther, E. Post, P. Convey, A. Menzel, C. Parmesan, T.J.C. Beebee, J.-M. Fromentin, O. Hoegh-Guldberg and F. Bairlein, Ecological responses to recent climate change. *Nature* 416 (2002) 389-395.
- [2] J.L. Valencia, A.S. Requejo, J.M. Gasco, A.M. Tarquis, A universal multifractal description applied to precipitation patterns of the Ebro River Basin, Spain. *Clim. Res.* 44 (2010) 17-25.
- [3] Q. Zhang, C.-Y. Xu, Z. Zhang, Y.D. Chen, C.-L. Liu, Spatial and temporal variability of precipitation maxima during 1960-2005 in the Yangtze River basin and possible association with large-scale circulation. *J. Hydrol.* 353 (2008) 215-227.
- [4] D. Schertzer and S. Lovejoy, Physical modeling and analysis of rain and clouds by anisotropic scaling of multiplicative processes. *J. Geophys. Res.* 92(D8) (1987) 9693-9714.
- [5] V.K. Gupta and E. Waymire, Multiscaling properties of spatial rainfall and river flow distributions. *J. Geophys. Res.* 95(D3) (1990) 1999-2009.
- [6] T.M. Over and V.K. Gupta, Statistical analysis of masoscale rainfall: dependence of a random cascade generator on large-scale forcing. *J. Appl. Meteorol.* 33 (1994) 1526-1542.
- [7] F. Schmitt, S. Vannitsem and A. Barbosa, Modeling of rainfall time series using two-state renewal processes and multifractals. *J. Geophys. Res.* 103(D18) (1998) 23181-23193.
- [8] C. Svensson, J. Olsson and R. Berndtsson, Multifractal properties of daily rainfall in two different climates. *Water Resour. Res.* 32(8) (1996) 2463-2472.
- [9] B. Sivakumar, Fractal analysis of rainfall observed in two different climatic regions. *Hydrol. Sci. J.* 45(5) (2000) 727-738.

- [10] C. De Michele and P. Bernardara, Spectral analysis and modeling of space-time rainfall fields. *Atmos. Res.* 77 (2005) 124-136.
- [11] J. Olsson, J. Niemczynowicz, and R. Berndtsson, Fractal analysis of high-resolution rainfall time series. *J. Geophys. Res.* 98(D12) (1993) 23265-23274.
- [12] V. Venugopal, S.G Roux., E. Foufoula-Georgiou and A. Arneodo, Revisiting multifractality of high-resolution temporal rainfall using a wavelet-based formalism. *Water Resour. Res.* 42 (2006) W06D14.
- [13] P. Molnar and P. Burlando, Variability in the scale properties of high resolution precipitation data in the Alpine climate of Switzerland. *Water Resour. Res.* 44(10) (2008) W10404.
- [14] G. Boni, A. Parodi and F. Siccaldi, A new parsimonious methodology of mapping the spatial variability of annual maximum rainfall in mountainous environments. *J. Hydrometeorol.* 9(3) (2008) 492-506.
- [15] D. Veneziano and P. Furcolo, Multifractality of rainfall and scaling of intensity-duration-frequency curves. *Water Resour. Res.* 38(12) (2002) 1306.
- [16] D. Veneziano, A. Langousis and P. Furcolo, Multifractality and rainfall extremes: A review. *Water Resour. Res.* 42 (2006) W06D15.
- [17] D. Veneziano and C. Lepore, The scaling of temporal rainfall. *Water Resour. Res.* 48 (2012) W08516.
- [18] Y. Tessier, S. Lovejoy and D. Schertzer, Universal multifractals: theory and observations for rain and clouds. *J. Appl. Meteorol.* 32(2) (1993) 223-250.
- [19] J. Olsson and J. Niemczynowicz, Multifractal analysis of daily spatial rainfall distributions. *J. Hydrol.* 187(1-2) (1996) 29-43.
- [20] S. Perica and E. Foufoula-Georgiou, Model for multiscale disaggregation of spatial rainfall based on coupling meteorological and scaling descriptions. *J. Geophys. Res.* 101 (D21) (1996) 26347-26341.
- [21] M. Menabde, D. Harris, A. Seed, G. Austin and D. Stow, Multiscaling properties of rainfall and bounded random cascades. *Water Resour. Res.* 33(12) (1997) 2823-2830.
- [22] G. Pandey, S. Lovejoy and D. Schertzer, Multifractal analysis of daily river flows including extremes for basins of five to two million square kilometres, one day to 75 years. *J. Hydrol.* 208(1-2) (1998) 62-81.
- [23] I. De Lima and J. Grasman, Multifractal analysis of 15-min and daily rainfall from a semi-arid region in Portugal. *J Hydrol.*, 220 (1999) 1-11.
- [24] R. Deidda, R. Benzi and F. Siccaldi, Multifractal modeling of anomalous scaling laws in rainfall. *Water Resour. Res.* 35 (6) (1999) 1853-1867.
- [25] M. Lilley, S. Lovejoy, N. Desaulniers-Soucy, D. Schertzer, Multifractal large number of drops limit in rain. *J. Hydrol.* 328 (2006) 20-37.
- [26] S. Lovejoy, D. Schertzer and V. Allaire, The remarkable wide range scaling of TRMM precipitation. *Atmos. Res.* 90 (2008) 10-32.
- [27] S. Lovejoy, J. Pinel, D. Schertzer, The global space-time cascade structure of precipitation: Satellites, gridded gauges and reanalyses. *Adv. Water Resour.* 45 (2012) 37-50.
- [28] A.P. Garcia-Marin, F.J. Jimenez-Hornero, and J.L. Ayuso-Munoz, Universal multifractal description of an hourly rainfall time series from a location in southern Spain. *Atmosfera* 21(4) (2008) 347-355.

- [29] F. Serinaldi, Multifractality, imperfect scaling and hydrological properties of rainfall time series simulated by continuous universal multifractal and discrete random cascade models. *Nonlin. Processes Geophys.* 17 (2010) 697-714.
- [30] T.C. Halsey, M.H. Jensen, L.P. Kadanoff, I. Procaccia and B.I. Schraiman, Fractal measures and their singularities: the characterization of strange sets. *Phys. Rev. A* 33 (1986) 1141-1151.
- [31] J.W. Kantelhardt, S.A. Zschiegner, E. Koscielny-Bunde, S. Havlin, A. Bunde and H.E. Stanley, Multifractal detrended fluctuation analysis of nonstationary time series. *Physica A* 316 (2002) 87-114.
- [32] C.K. Peng, S.V. Buldyrev, A.L. Goldberger, S. Havlin, F. Sciortino, M. Simons, and H.E. Stanley, Long-range correlations in nucleotide sequences. *Nature* 356 (1992) 168-170.
- [33] C.K. Peng, S.V. Buldyrev, S. Havlin, M. Simons, H.E. Stanley and A.L. Goldberger, Mosaic organization of DNA nucleotides. *Phys. Rev. E* 49 (1994) 1685-1689.
- [34] Z.G. Yu, V. Anh and B. Wang, Correlation property of length sequences based on global structure of complete genome. *Phys. Rev. E* 63 (2001) 011903.
- [35] Z.G. Yu, V.V. Anh, K.S. Lau and L.Q. Zhou, Fractal and multifractal analysis of hydrophobic free energies and solvent accessibilities in proteins. *Phys. Rev. E* 73 (2006) 031920.
- [36] C. Matsoukas, S. Islam, I. Rodriguez-Iturbe, Detrended fluctuation analysis of rainfall and streamflow time series. *J. Geophys. Res.* 105 (D23) (2000) 29165-29172.
- [37] J.W. Kantelhardt, D. Rybski, S.A. Zschiegner, P. Braun, E. Koscielny-Bunde, V. Livina, S. Havlin and A. Bunde, Multifractality of river runoff and precipitation: comparison of fluctuation analysis and wavelet methods. *Physica A* 330 (1-2) (2003) 240-245.
- [38] J.W. Kantelhardt, E. Koscielny-Bunde, D. Rybski, P. Braun, A. Bunde and S. Havlin, Long-term persistence and multifractality of precipitation and river runoff records. *J. Geophys. Res.* 111(D1) (2006) D01106.
- [39] E. Koscielny-Bunde, J.W. Kantelhardt, P. Braun, A. Bunde and S. Havlin, Longterm persistence and multifractality of river runoff records: Detrended fluctuation studies. *J. Hydrol.* 322(1-4) (2006) 120-137.
- [40] Z.W. Li and Y.K. Zhang, Quantifying fractal dynamics of groundwater systems with detrended fluctuation analysis, *J. Hydrol.* 336(1-2) (2007) 139-146.
- [41] V. Anh, Z.G. Yu and J.A. Wanliss, Analysis of global geomagnetic variability. *Nonlin. Processes Geophys.* 14(6) (2007) 701-708.
- [42] V.V. Anh, J.M. Yong and Z.G. Yu, Stochastic modeling of the auroral electrojet index. *J. Geophys. Res.* 113 (2008) A10215.
- [43] Q. Zhang, C.-Y. Xu, Z.G. Yu, C.-L. Liu, Y.D. Chen, Multifractal analysis of streamflow records of the East River basin (Pearl River), China. *Physica A* 388 (2009) 927-934.
- [44] Q. Zhang, Z.G. Yu, C.-Y. Xu, V. Anh, Multifractal analysis of measure representation of flood/drought grade series in the Yangtze Delta, China, during the past millennium and their fractal model simulation. *Int. J. Climatol.* 30 (2010) 450-457.
- [45] Z.G. Yu, V. Anh and R. Eastes, Multifractal analysis of geomagnetic storm and solar flare indices and their class dependence. *J. Geophys. Res.* 114 (2009) A05214.
- [46] Z.G. Yu, V. Anh, Y. Wang, D. Mao and J. Wanliss, Modeling and simulation of the horizontal component of the geomagnetic field by fractional stochastic differential equations in conjunction with empirical mode decomposition. *J. Geophys. Res.* 115 (2010) A10219.

- [47] Q. Zhang, C.Y. Xu, S. Becker, Z.X. Zhang, Y.Q. Chen, M. Coulibaly, Trends and abrupt changes of precipitation maxima extremes in the Pearl River basin, China. *Atmos. Sci. Lett.* 10 (2009) 132C144.
- [48] M. Gemmer, T. Fischer, B. Su, L.L. Liu, Trends of precipitation extremes in the Zhujiang River Basin, South China. *J. Clim.* 24 (2011)750C761
- [49] V. Anh, K.S. Lau and Z.G. Yu, Multifractal characterisation of complete genomes. *J. Phys. A: Math. Gen.* 34(36) (2001) 7127-1739.
- [50] F. Schmitt, D. Lavalée, D. Schertzer and S. Lovejoy, Empirical determination of universal multifractal exponents in turbulent velocity fields. *Phys. Rev. Lett.*, 68 (1992) 305-308.
- [51] D. Lavalée, S. Lovejoy, D. Schertzer and P. Ladoy, Nonlinear variability and landscape topography: analysis and simulation. In: *Fractals in Geography* (N. Lam and L. De Cola, Eds.) Prentice Hall, Englewood Cliffs, p158-192, 1993.
- [52] Z.G. Yu, V. Anh, R. Eastes and D.L. Wang, Multifractal analysis of solar flare indices and their horizontal visibility graphs. *Nonlin. Processes Geophys.* 19 (2012) 657-669.
- [53] M.S. Movahed, G.R. Jafari, F. Ghasemi, S. Rahvar and M.R.R. Tabar, Multifractal detrended fluctuation analysis of sunspot time series. *J. Stat. Mech.: Theory Exper.* 2 (2006) P02003.
- [54] S. Havlin, R. Selinger, M. Schwartz, H.E. Stanley, and A. Bunde, Random multiplicative processes and transport in structures with correlated spatial disorder. *Phys. Rev. Lett.* 61(13) (1988) 1438-1441.
- [55] Y. Zhou, Y. Leung and Z.G. Yu, Relationships of exponents in multifractal detrended fluctuation analysis and conventional multifractal analysis. *Chin. Phys. B* 20(9) (2011) 090507.
- [56] A.J. Lawrence, N.T. Kottegoda, Stochastic modeling of riverflow time series. *J. R. Stat. Soc., Ser. A (General)* 140 (1) (1977) 1-47.
- [57] E. Kocielny-Bunde, A. Bunde, S. Havlin, Y. Goldreich, Analysis of daily temperature fluctuations. *Physica A* 231 (1996) 393-396.
- [58] V. Livina, Y. Ashkenazy, Z. Kizner, V. Strygin, A. Bunde, S. Halvin, A stochastic model of river discharge fluctuations. *Physica A* 330 (2003) 283-290.
- [59] J. Niu, Precipitation in the Pearl River basin, South China: scaling, regional patterns, and influence of large-scale climate anomalies. *Stoch. Environ. Res. Risk Assess.* 27 (2013) 1253-1268.

Table 1: The geographical information of the rainfall stations and estimated multifractal parameters of the daily rainfall data in Pearl River basin. We list the stations according to the decreasing order of their elevations.

Group	Station name	Long. (°)	Lat. (°)	Elev. (m)	α	$h(1)$	$\Delta h(q)$	$h(2)$	$K(2)$	$K'(2)$
Group 1 (with Elev. $\geq 1000\text{m}$)	56691	104.28	26.87	2237.5	0.9905	0.7239	0.4602	0.6106	0.1780	0.2266
	56786	103.83	25.58	1998.7	1.2019	0.7279	0.6758	0.5666	0.1970	0.3226
	56875	102.55	24.33	1716.9	0.9807	0.7898	0.8851	0.5248	0.1951	0.5300
	56886	103.77	24.53	1704.3	0.9563	0.7560	0.7340	0.5615	0.1877	0.3890
	57806	105.90	26.25	1431.1	1.1437	0.6958	0.3929	0.5978	0.1886	0.1960
	57902	105.18	25.43	1378.5	1.0583	0.6908	0.4169	0.5797	0.1874	0.2222
	56985	103.38	23.38	1300.7	0.9451	0.7567	0.4517	0.5805	0.2159	0.3524
	57922	107.55	25.83	1013.3	1.1786	0.6932	0.3905	0.5902	0.1919	0.2060
Group 2 (with Elev. between 200m to 1000m)	59209	105.83	23.42	794.10	1.0300	0.7271	0.5094	0.5717	0.1745	0.3108
	59218	106.42	23.13	739.90	1.1541	0.7188	0.6016	0.5779	0.1697	0.2818
	57906	106.08	25.18	566.80	0.9873	0.7125	0.4786	0.5816	0.2072	0.2618
	59021	107.03	24.55	484.60	0.8460	0.6927	0.5752	0.5515	0.2009	0.2824
	57916	106.77	25.43	440.30	0.9970	0.7324	0.6086	0.5714	0.2105	0.3220
	59102	115.65	24.95	303.90	1.0614	0.7619	0.6160	0.6034	0.2184	0.3170
	57932	108.53	25.97	285.70	1.0908	0.7102	0.5882	0.5807	0.2045	0.2590
	59096	114.48	24.37	214.80	1.0230	0.7622	0.5354	0.6279	0.2145	0.2686
Group 3 (with Elev. $\leq 200\text{m}$)	59211	106.60	23.90	173.50	0.7283	0.7395	0.5026	0.5893	0.2222	0.3004
	59037	108.10	23.93	170.80	1.2448	0.7338	0.5106	0.6168	0.2316	0.2340
	57957	110.30	25.32	164.40	0.8394	0.7308	0.7217	0.5804	0.2192	0.3008
	59058	110.52	24.20	145.70	1.0215	0.7190	0.3825	0.6176	0.1916	0.2028
	57996	114.32	25.13	133.80	0.8723	0.7465	0.5241	0.6200	0.1991	0.2530
	59417	106.85	22.33	128.80	1.4062	0.7411	0.5340	0.6131	0.1880	0.2560
	59431	108.22	22.63	121.60	1.1208	0.7404	0.4751	0.6208	0.2169	0.2392
	57947	109.40	25.22	121.30	0.8441	0.7265	0.5512	0.5933	0.2393	0.2664
	59265	111.30	23.48	114.80	1.4781	0.7321	0.5647	0.5843	0.2116	0.2956
	59065	111.53	24.42	108.80	0.8759	0.7425	0.4271	0.6272	0.1996	0.2306
	59072	112.38	24.78	98.30	1.0028	0.7403	0.4047	0.6287	0.1949	0.2232
	59046	109.40	24.35	96.80	0.8041	0.7196	0.6851	0.5592	0.2191	0.3208
	59242	109.23	23.75	84.90	0.7554	0.7342	0.5614	0.6077	0.2200	0.2530
	59087	113.53	23.87	68.60	1.1332	0.7595	0.6136	0.6126	0.2201	0.2938
	59082	113.60	24.68	61.00	0.9246	0.7466	0.6232	0.6155	0.2060	0.2622
	59271	112.43	23.63	57.30	1.2472	0.7295	0.5859	0.5820	0.1889	0.2950
	59462	111.57	22.77	53.30	1.3551	0.7411	0.5056	0.5901	0.2097	0.3020
	59254	110.08	23.40	42.50	0.7011	0.7496	0.3724	0.6436	0.1978	0.2120
	59278	112.45	23.03	41.00	1.6072	0.7472	0.7785	0.5413	0.1945	0.4118
	59287	113.33	23.17	41.00	1.1680	0.7467	0.6313	0.5675	0.2113	0.3584
59293	114.68	23.73	40.60	0.9206	0.7711	0.5821	0.6040	0.2570	0.3342	
59294	113.83	23.33	38.90	0.6213	0.7641	0.7561	0.5460	0.2104	0.4362	
59478	112.78	22.25	32.70	0.8213	0.7829	0.6593	0.6031	0.2476	0.3596	
59298	114.42	23.08	22.40	0.7185	0.7566	0.6993	0.5558	0.2308	0.4016	
59493	114.10	22.55	18.20	1.1102	0.7695	0.7200	0.5552	0.2600	0.4286	
mean \pm std					1.0236 ± 0.2141	0.7381 ± 0.0234	0.5681 ± 0.1210	0.5891 ± 0.0275	0.2080 ± 0.0205	0.2980 ± 0.0728

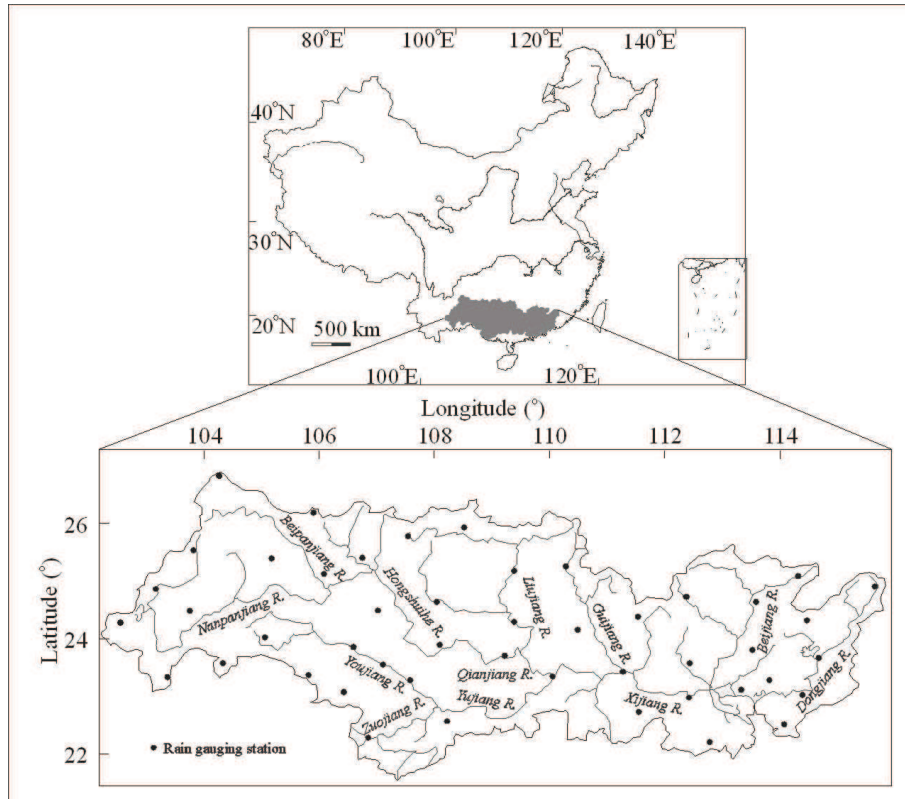


Figure 1: Location of the rain gauge stations in the Pearl River basin, China.

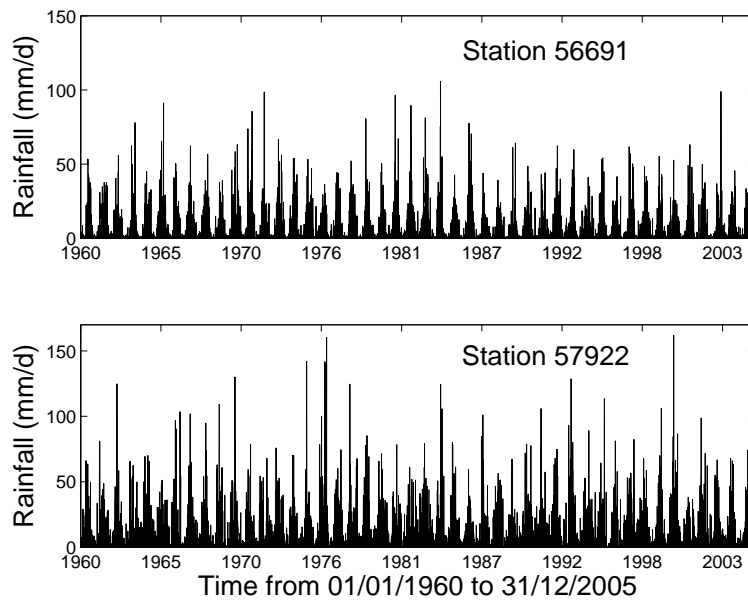


Figure 2: The daily rainfall data of station 56691 and Station 57922 in the Pearl River basin over the entire study period.

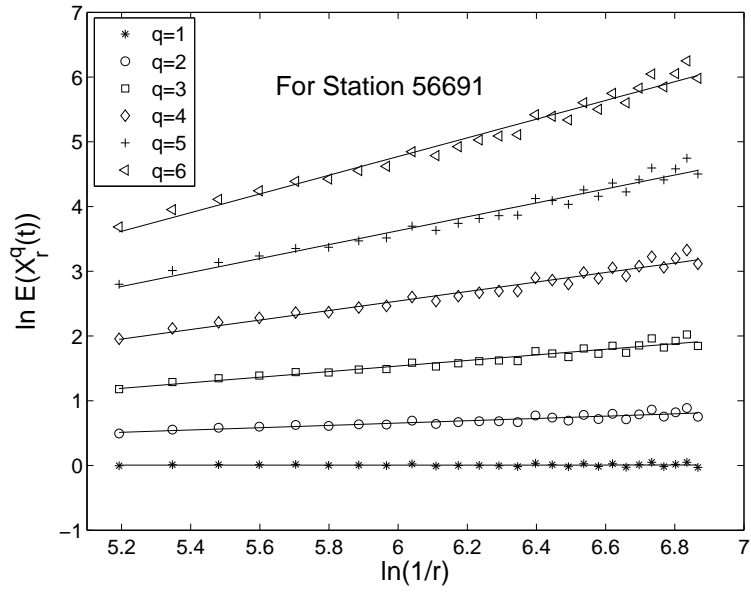


Figure 3: An example for obtaining the empirical $K(q)$ curve.

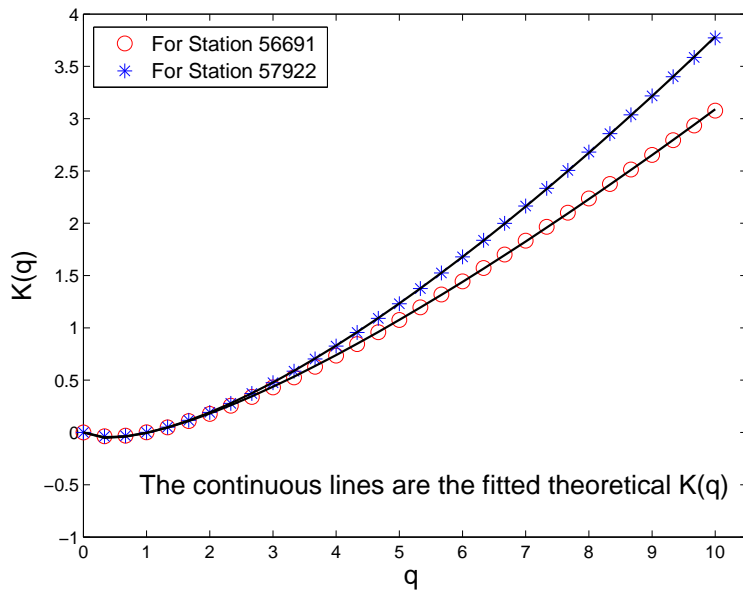


Figure 4: The $K(q)$ curves of daily rainfall data in two stations (the dotted curves), and their fitted curves (continuous lines) by the universal multifractal model.

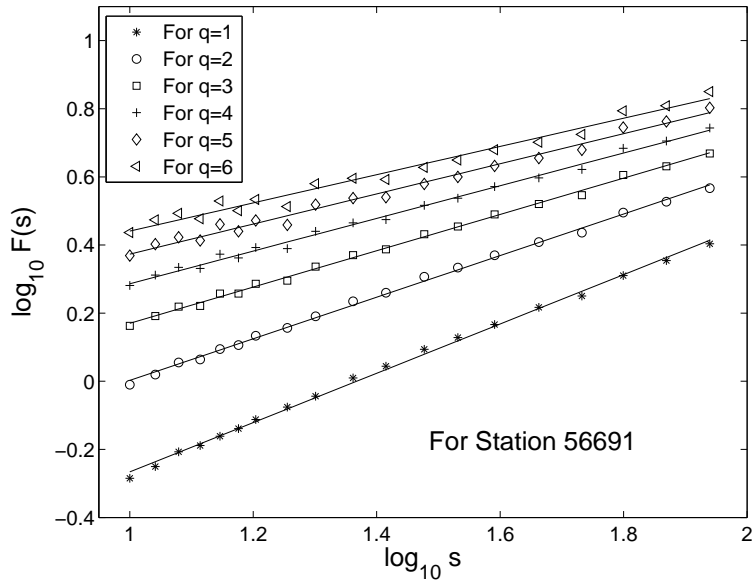


Figure 5: An example for obtaining the empirical $h(q)$ curve.

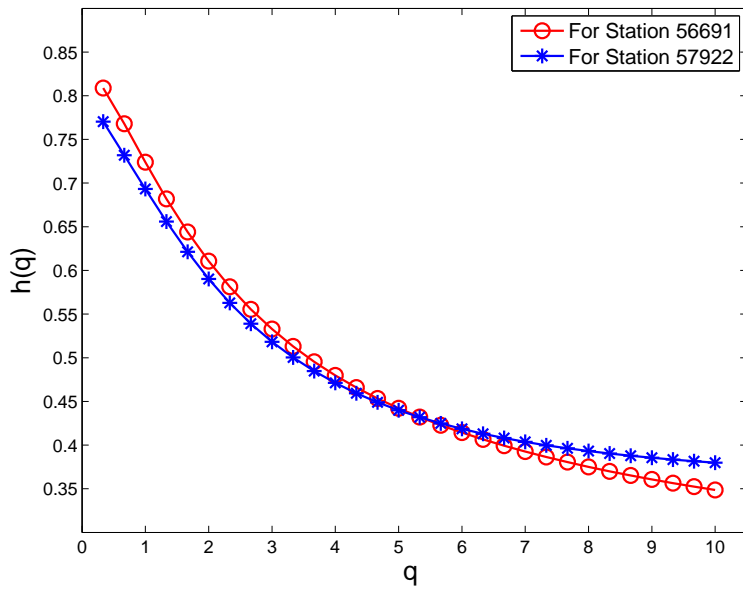


Figure 6: The $h(q)$ curves of daily rainfall data in two stations.

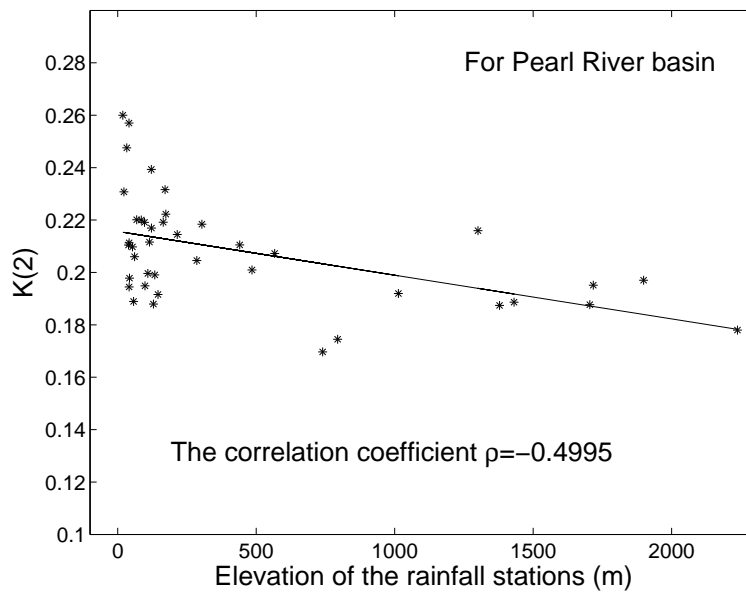


Figure 7: The correlation relationship between the elevation of the rainfall stations and the $K(2)$ value of the rainfall time series for the Pearl River basin.